

Tb(III) Functionalized Vesicles for Phosphate Sensing: Membrane Fluidity Controls the Sensitivity

Supratim Banerjee, Mouchumi Bhuyan and Burkhard König*

Institut für Organische Chemie, Universität Regensburg, D-93040 Regensburg, Germany

E-mail: Burkhard.koenig@chemie.uni-regensburg.de

Table of Contents

General methods and materials.....	S2
Synthetic scheme.....	S2
Preparation of Vesicles.....	S9
Receptor concentration on the vesicle surface.....	S9
Dynamic Light Scattering (DLS) of vesicles.....	S10
Sensing mechanism.....	S11
Sensitivity/response of vesicles.....	S12
Emission spectra.....	S13
Excitation spectra.....	S17
Sensing of α -Casein.....	S18
Size Exclusion Chromatography (SEC).....	S19
Hill equation.....	S19
Non-linear fitting curves for different analytes (DPPC vesicles, 25 °C).....	S20
Comparison of binding constants of UTP and ATP between DSPC and DPPC vesicles at 25 °C.....	S23
Non-linear fitting curve for UTP against a DPPC vesicle (25 °C) after SEC.....	S23
Non-linear fitting curves at other temperatures.....	S24

General methods and materials

Thin layer chromatography (TLC) analyses were performed on silica gel 60 F-254 with a 0.2 mm layer thickness. Detection via UV light at 254 nm / 365 nm or through staining with ninhydrin in EtOH. Column chromatography was performed on silica gel (70–230 mesh) from Merck. Commercially available solvents of standard quality were used. All reagent-grade chemicals were used without further purification unless otherwise specified. Phospholipids were purchased from Avanti Polar Lipids Inc. NMR spectra were recorded on Bruker Avance 300 and 600 (1H: 300.1 and 600.2 MHz, 13C: 75.5 and 150.95 MHz, T = 300 K). The chemical shifts are reported in δ [ppm] relative to external standards (solvent residual peak). Mass spectra were measured on Varian CH-5 (EI), Finnigan MAT 95 (CI; FAB and FD), Finnigan MAT TSQ 7000 (ESI) with Xenon as ionization gas for FAB. IR spectra were recorded with a JASCO FT/IR-430 spectrometer.

Luminescence spectra were recorded on a Varian ‘Cary Eclipse’ fluorescence spectrophotometer with temperature control using 1 cm quartz cuvettes (Hellma). The spectra were recorded in phosphorescence mode using the following parameters: total decay time (s) = 0.02; no of flashes = 1; delay time = 0.1 ms; gate time = 5 ms. Absorption spectra were recorded on a Varian Cary BIO 50 UV/VIS/NIR Spectrometer equipped with a temperature control using 1 cm quartz cuvettes (Hellma). PCS measurements were performed on a Malvern Zetasizer Nano at 25 °C using 1 cm disposable polystyrene cuvettes (VWR).

Synthetic Scheme

Synthesis of Zn₂Trp

The amphiphilic **Zn₂Trp** complex was synthesized starting from **1**. The synthesis of **1** was previously reported by us.¹ In the first step, **1** was coupled with **2**² through an aromatic nucleophilic substitution to obtain **3**. The *t*-Boc groups in **3** were then deprotected with TFA in DCM to furnish **4**. In the final step, **4** was refluxed in MeOH in the presence of Zn(ClO₄)₂ to obtain **Zn₂Trp**.

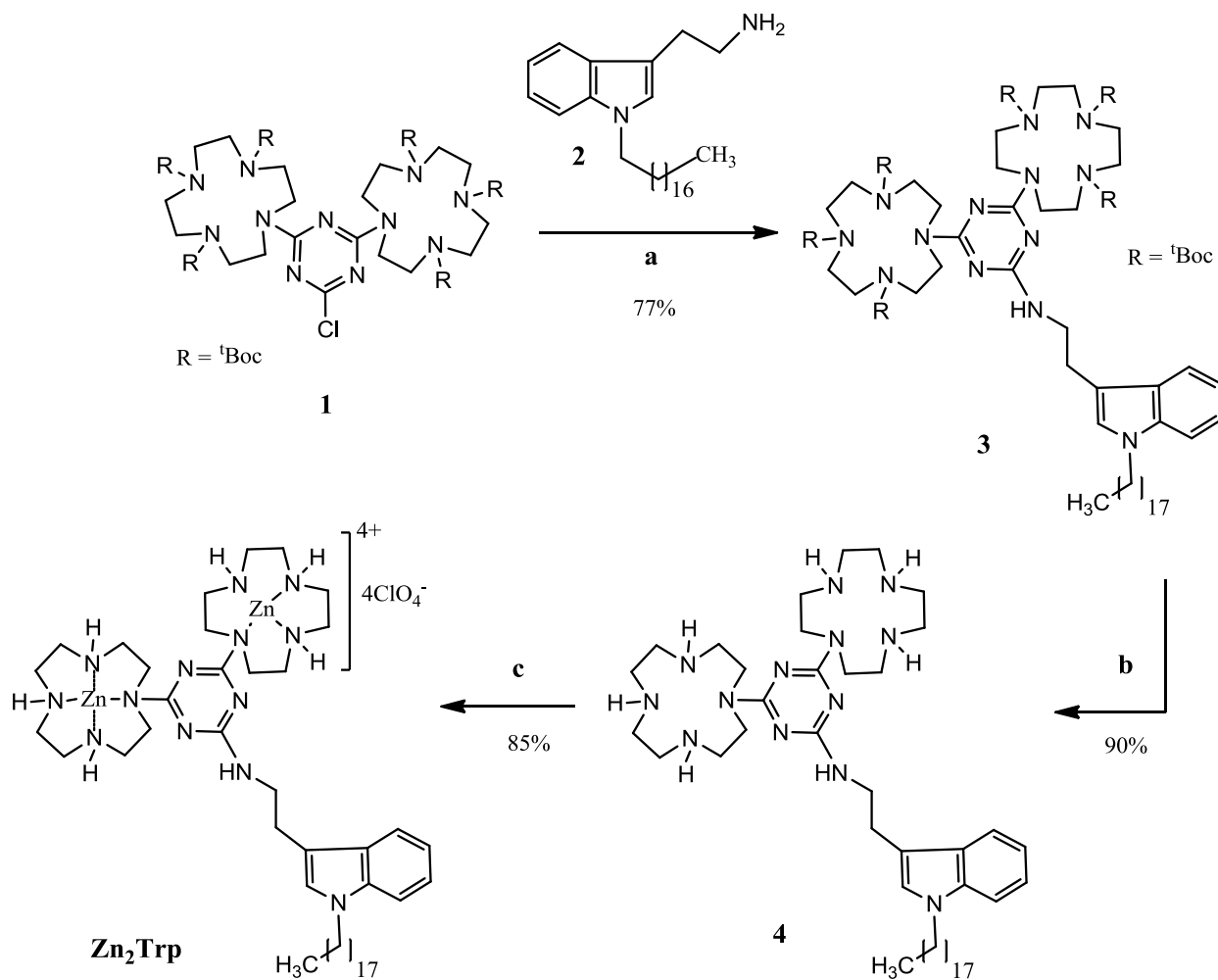


Figure S1. Synthesis of **Zn₂Trp**: a) K₂CO₃, dioxane, 90 °C; b) TFA, DCM, rt; c) Zn(ClO₄)₂, MeOH, 65 °C.

Synthesis of compound 3

Compound **1** (165 mg, 0.155 mmol, 1eq) and **2** (90 mg, 0.218 mmol, 1.4 eq) were taken in a 10 mL round bottom flask and 1,4-dioxane (2 mL) was added to it. In the suspension stirred at room temperature, anhydrous K₂CO₃ (64 mg, 0.46 mmol, 3 eq) was added. The reaction mixture was then kept for stirring at 90 °C for 12 h. The solvent was subsequently removed under high vacuum and the crude product was purified by a silica gel column (30% EA/PE; R_f = 0.4). Compound **3** was obtained as a white solid (175 mg, yield 77%).

MP: 96-98°C.

¹H NMR (CDCl₃/300 MHz): 0.87 (t, J = 6 Hz, 3H), 1.22-1.27 (m, 28H), 1.41 (s, 18H), 1.45 (s, 36 H), 1.64 (br s, 2H), 1.8 (t, J = 6 Hz, 2H), 2.32-2.22 (m, 2H), 2.96 (t, J = 7.5 Hz, 2H), 3.4-3.7 (m, 32 H), 4.06 (t, J = 7.5 Hz, 2H), 6.93 (s, 1H), 7.09-7.05 (m, 1H), 7.22-7.17 (m, 1H), 7.3 (d, J = 9 Hz, 1H), 7.56 (d, J = 9 Hz, 1H).

¹³C NMR (CDCl₃/75 MHz): 14.14, 22.71, 25.88, 27.09, 28.47, 28.54, 29.31, 29.38, 29.44, 29.62, 29.71, 30.37, 31.94, 41.23, 46.30, 50.24, 79.71, 109.43, 111.75, 118.68, 118.93, 121.47, 125.75, 127.92, 136.40, 156.47, 165.76.

IR (ATR) [cm⁻¹]: 2920, 2852, 1688, 1535, 1465, 1406, 1361, 1244, 1155, 852.

MS (ESI(+), DCM-MeOH + 10 mM NH₄OAc): m/z = 1433.1 [M+H⁺]⁺ (calc. 1433.02), FW of C₇₇H₁₃₃N₁₃O₁₂: 1432.01.

Synthesis of compound 4

Compound **3** (140 mg, 0.095 mmol) was taken in a 10 mL round bottom flask and dissolved in DCM (3 mL). Then TFA (730 μL, 9.5 mmol) was added to it and the reaction mixture was stirred at room temperature for 3 h. The solvent and other volatiles were removed thereafter under high vacuum to obtain a brownish solid as a crude product. It was dissolved in 8:2 H₂O-MeOH and passed through a basic ion-exchange resin (the resin was swelled in the same solvent mixture for 15 min prior to use). The fractions with pH>10 were combined; MeOH was removed in rotary evaporator and then lyophilized. The product **4** was obtained as a light brownish solid (68 mg, yield 85%).

MP: 146-148°C

¹H NMR (CDCl₃/300 MHz): 0.87 (t, J = 6 Hz, 3H), 1.22-1.32 (m, 28H), 1.8 (t, J = 7.5 Hz, 2H), 2.65-2.89 (m, 2H), 2.99 (t, J = 7.5 Hz, 2H), 3.4-3.7 (m, 32 H), 4.06 (t, J = 7.5 Hz, 2H), 6.93 (s, 1H), 7.09-7.05 (m, 1H), 7.22-7.17 (m, 1H), 7.3 (d, J = 9 Hz, 1H), 7.56 (d, J = 9 Hz, 1H).

¹³C NMR (CDCl₃/75 MHz): 14.14, 22.7, 26.00, 27.08, 29.30, 29.37, 29.53, 29.67, 29.71, 30.32, 31.93, 32.01, 41.22, 41.33, 46.25, 48.28, 48.82, 109.41, 11.97, 118.58, 119.04, 121.37, 125.77, 127.59, 127.93, 136.37, 165.64, 166.79.

IR (ATR) [cm⁻¹]: 2920, 2850, 1533, 1486, 1412, 1359, 1007, 904, 812.

MS (ESI(+), DCM–MeOH + 10 mM NH₄OAc): $m/z = 433.5 [M+2NH_4^+]^{2+}$ (calc. 433.8), 289.3
 $[M+H^++NH_4^+]^{2+}$ (calc. 289.6); FW of C₄₇H₈₅N₁₃: 831.7.

Synthesis of Zn₂Trp

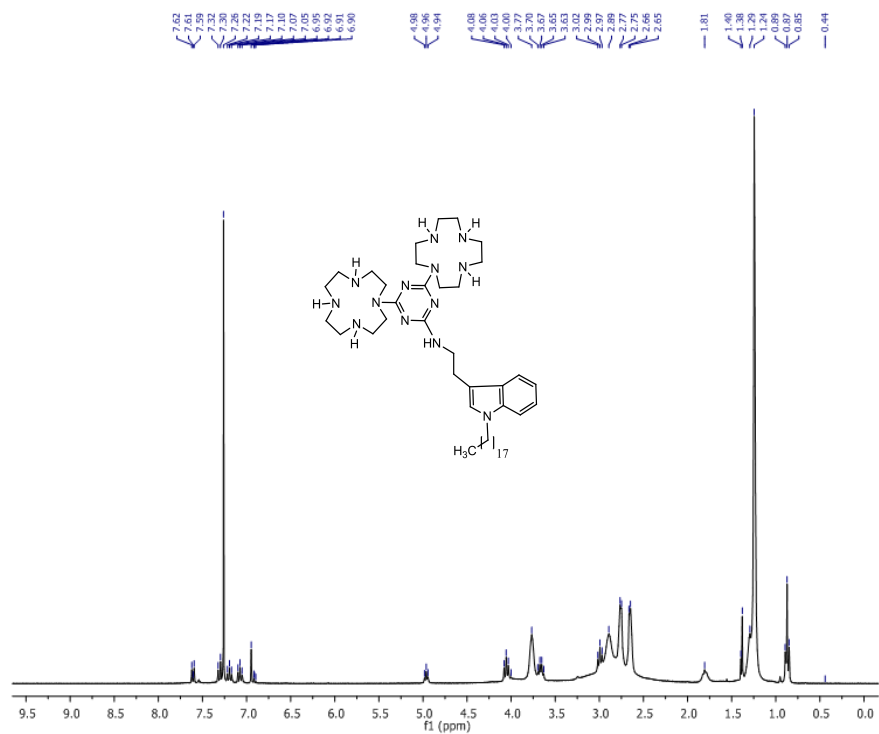
45 mg of compound **4** (0.054 mmol, 1 eq) was dissolved in 2 mL of MeOH. Zn(ClO₄)₂ · 6 H₂O (44 mg, 0.118 mmol, 2.2 eq) was added to it. A precipitate appeared immediately which dissolved upon heating to 65 °C. The reaction mixture was stirred at this temperature for 24 hr. The solvent was removed under high vacuum and a slightly brownish solid was obtained. CHCl₃ was added to it and filtered. After evaporation of CHCl₃ from the filtrate, water (3 mL) was added to it and lyophilized. A yellowish, hygroscopic solid was obtained (63 mg, yield 85%).

¹H NMR (CDCl₃-CD₃OD (1:1)/600 MHz): 0.89 (t, J = 6 Hz, 3H), 1.22-1.29 (m, 28H), 1.74 (br, 2H), 2.69-3.67 (m, 32H), 4.04 (t, J = 6 Hz, 2H), 6.98 (s, 1H), 7.04-7.01 (m, 1H), 7.11-7.15 (m, 1H), 7.27-7.29 (m, 1H), 7.54-7.56 (m, 1H).

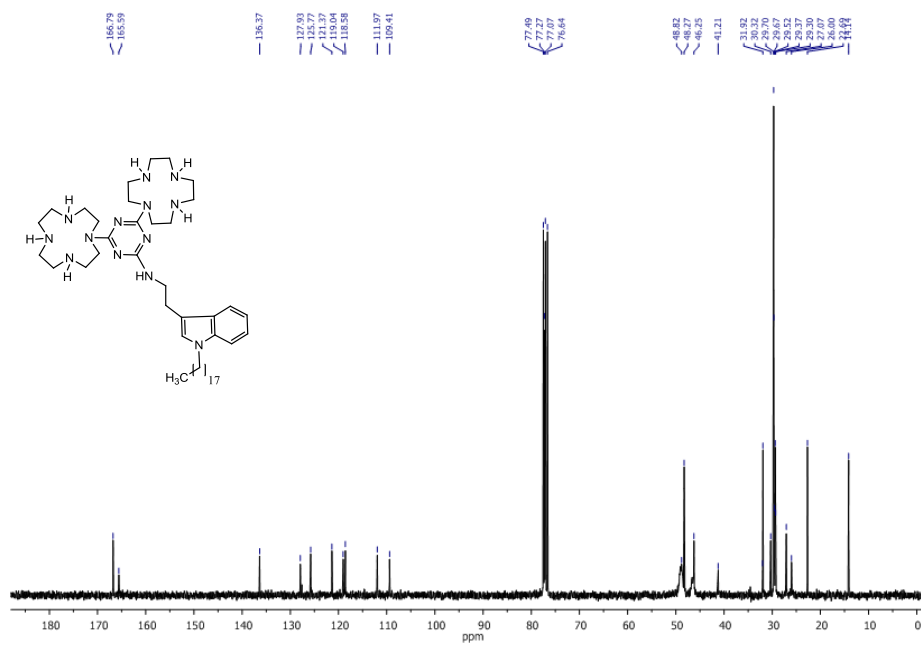
¹³C NMR (CDCl₃-CD₃OD (1:1) /150 MHz): 14.25, 23.08, 25.32, 26.01, 27.41, 27.44, 29.47, 29.78, 29.97, 30.02, 30.07, 30.10, 30.83, 32.36, 48.71, 48.86, 49.00, 49.14, 49.28, 58.42, 109.99, 111.84, 111.90, 118.98, 119.26, 121.77, 126.82, 128.44, 136.92, 166.12, 166.36, 171.15, 170.79.

MS (ESI(+), DCM–MeOH + 10 mM NH₄OAc): $m/z = 538.9 [M^{4+} + 2CH_3CO_2^-]^{2+}$ (calc. 538.8),
FW of C₄₇H₈₅N₁₃Zn₂: 959.5.

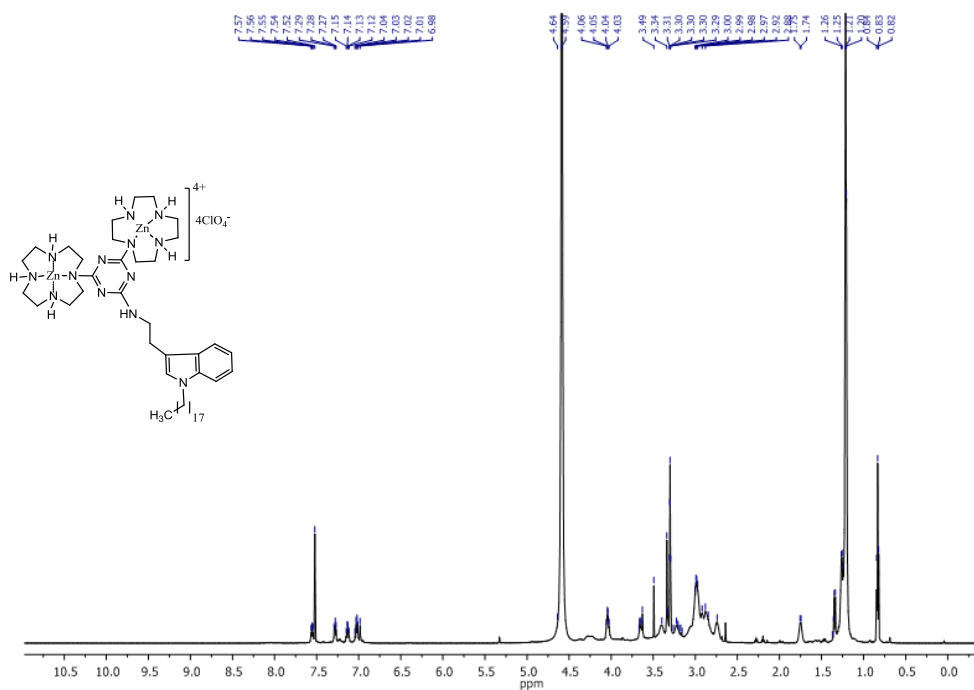
^1H NMR of compound 4 (CDCl_3 , 300 MHz)



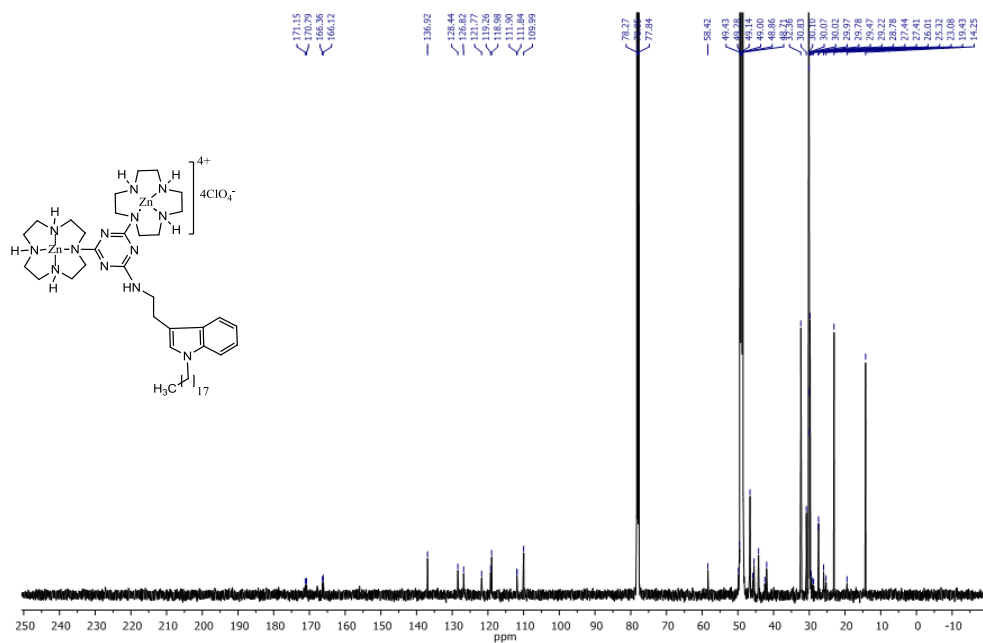
^{13}C NMR of compound 4 (CDCl_3 , 75 MHz)



^1H NMR of Zn_2Trp (1:1 $\text{CDCl}_3\text{-CD}_3\text{OD}$, 600 MHz)



^{13}C NMR of Zn_2Trp (1:1 $\text{CDCl}_3\text{-CD}_3\text{OD}$, 150 MHz)



Synthesis of Tb-1

Tb-1 was synthesized following a literature procedure.³

Synthesis of Zn₂-C18

Zn₂-C18 was synthesized following a literature procedure previously reported by us.⁴

Synthesis of Tb-2

Tb-2 was synthesized following a literature procedure reported by us.²

Preparation of vesicles

In small glass reaction vessels, required volumes of solutions of the lipid (9.6 mM in CHCl₃), **Zn₂Trp** (1 mM in 1:1 CHCl₃/MeOH) and **Tb-1** (1 mM in 1: 1 CHCl₃/MeOH) were mixed. After evaporation of the organic solvents, HEPES buffer solution (25 mM, pH = 7.4) was added to them. The samples were then heated above the phase transition temperatures of the lipids (75°C, 65°C and 45°C for DSPC, DPPC and DMPC, respectively) for 15 min to obtain slightly turbid multi-lamellar vesicle suspensions. Small uni-lamellar dispersions were obtained by extrusion (at the aforementioned temperatures for the respective lipids) through 100 nm-pore size polycarbonate membranes with a LiposoFast liposome extruder from Avestin. The extruded samples were diluted 5 times to obtain vesicles with the desired concentrations which were used for all the studies. The standard size distribution of vesicles after extrusion is shown in fig. S2-S4.

Receptor concentration on the vesicle surface

Assuming that the receptors distribute equally in the outer and inner surface⁵ (excluding the possibility of flipping of the highly charged zinc-cyclen through the membrane), and the thickness of the bilayer as 5 nm,⁶ the ratio of the outer and inner surface receptors for the 100 nm vesicles would be ~ 1:1. This corresponds to a concentration of 1.0×10^{-5} mol/L of **Zn₂Trp** available for the binding.

Dynamic Light Scattering measurements

Results

	Size (r.nm):	% Intensity	Width (r.nm)
Z-Average (r.nm): 53,35	Peak 1: 59,73	100,0	20,73
Pdl: 0,097	Peak 2: 0,000	0,0	0,000
Intercept: 0,911	Peak 3: 0,000	0,0	0,000

Result quality Good

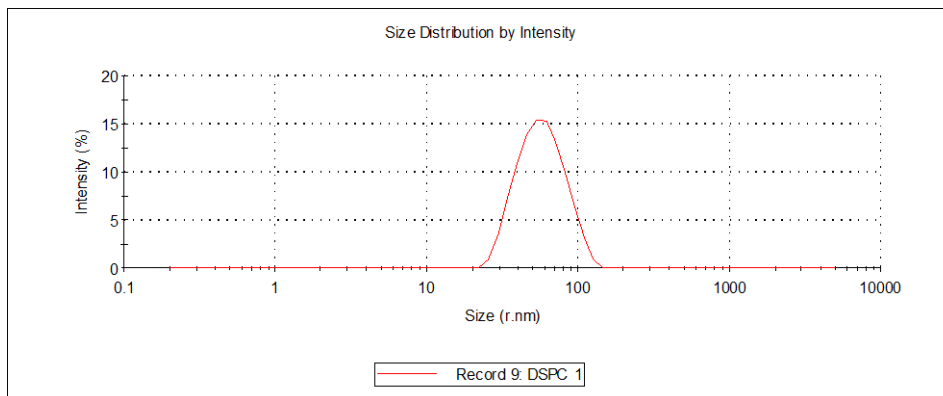


Figure S2. The size distribution of a DSPC vesicle sample: DSPC (1.6×10^{-4} M)/Zn₂Trp (2×10^{-5} M)/Tb-1 (2×10^{-5} M).

Results

	Size (r.nm):	% Intensity	Width (r.nm)
Z-Average (r.nm): 53,15	Peak 1: 59,03	100,0	19,18
Pdl: 0,101	Peak 2: 0,000	0,0	0,000
Intercept: 0,897	Peak 3: 0,000	0,0	0,000

Result quality Good

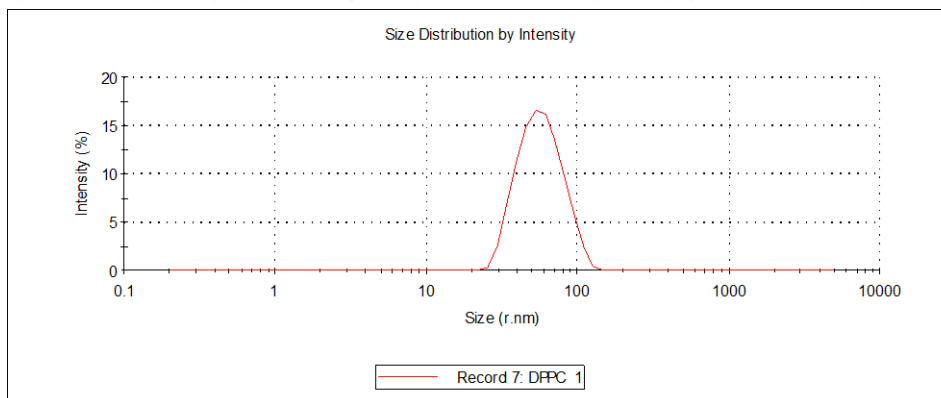


Figure S3. The size distribution of a DPPC vesicle sample: DPPC (1.6×10^{-4} M)/Zn₂Trp (2×10^{-5} M)/Tb-1 (2×10^{-5} M).

Results

	Size (r.nm):	% Intensity	Width (r.nm)
Z-Average (r.nm): 52,85	Peak 1: 58,20	100,0	18,55
Pdl: 0,112	Peak 2: 0,000	0,0	0,000
Intercept: 0,900	Peak 3: 0,000	0,0	0,000

Result quality Good

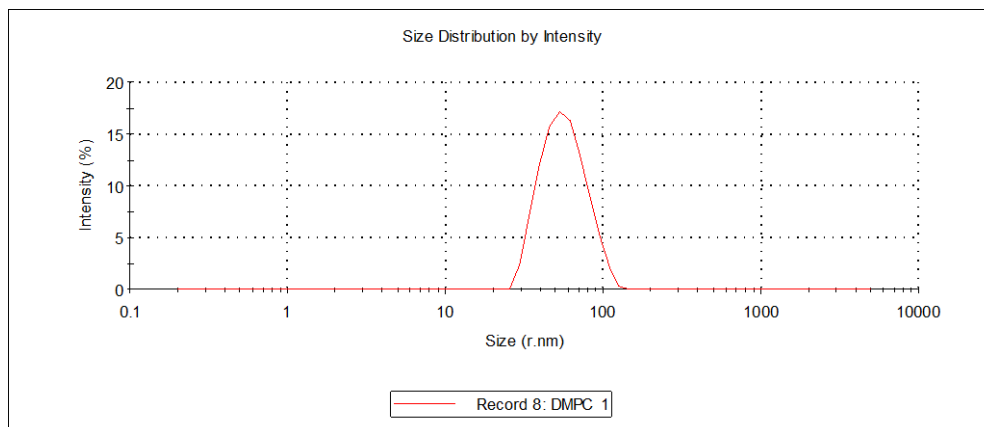


Figure S4. The size distribution of a DMPC vesicle sample: DMPC (1.6×10^{-4} M)/**Zn₂Trp** (2×10^{-5} M)/**Tb-1** (2×10^{-5} M).

Sensing mechanism

Co-embedding of **Zn₂Trp** and **Tb-1** in the vesicles leads to the formation of self-assembled mixed patches/domains in the bilayer membrane and results in an efficient sensitization of Tb(III) due to its proximity to the sensitizer. The binding of phosphate anions brings about a change in the solvation and charge density in the local environment of the receptors. This disrupts the self-assembled patches and the components are reorganized in the vesicular membrane leading to a higher separation of the Tb(III) from the receptor-sensitizer. We have previously utilized such analyte induced disassembly of patches for the design of fluorescent vesicular chemosensors where environment sensitive dyes, upon expulsion from the patches, exhibited emission changes.⁴

Sensitivity/response of the Vesicles

The initial intensity varied from sample to sample (even for samples with the same compositions). Therefore, we correlated the sensitivity/response (S_v) of the vesicles to $(I_0-I)/I_0$ [I_0 = initial emission intensity] of the embedded Tb(III) at each stage of analyte addition and it is thus independent of the absolute value of initial intensity. This allowed a convenient way to compare the sensitivity of different vesicle samples. For example, DPPC vesicles (at 25 °C) typically exhibited S_v ~50-60% for the nucleotide triphosphates (ATP, UTP, GTP) and for PP_i (when the saturation point was reached) whereas DSPC vesicles exhibited only 30-35% changes for the same analytes at this temperature. Although, the binding constants are comparable for these two vesicles but data for the DPPC vesicles have a better signal to noise (S/N) ratio and hence they are chosen for the measurements at 25°C. At a higher temperature (37 °C), however, S_v increases to 45-50% for DSPC vesicles (more fluidic at this temperature). In case of DMPC ($T_m = 23^\circ\text{C}$) vesicles, the measurements were done at 25°C (just above the T_m) and 15 °C (below T_m). The highly fluidic DMPC vesicles at 25°C exhibited very poor sensitivity towards analytes ($S_v \sim 5-10\%$). However, the sensitivity increased significantly upon decreasing the fluidity to 15°C ($S_v \sim 60-70\%$). The changes in emission intensity in binding titrations for different vesicles samples at various temperatures are listed in table S1.

Table S1: Changes in emission intensity of vesicles; ^a the values are at the saturation points for each titration

Lipid (temperature)	Analyte	^a $(I_0-I)/I_0$
1. DPPC (25 °C)	UTP, ATP, GTP, PP_i	50-60 %
	ADP, pSer, AMP	40-50 %
2. DSPC (25 °C)	UTP, ATP, GTP, PP_i	30-35 %
	ADP, pSer, AMP	25-30 %
DSPC (37 °C)	UTP, ATP	45-50 %
3. DMPC (25 °C)	UTP, ATP	5-10 %
DMPC (15 °C)	UTP, ATP	60-70 %

Emission Spectra

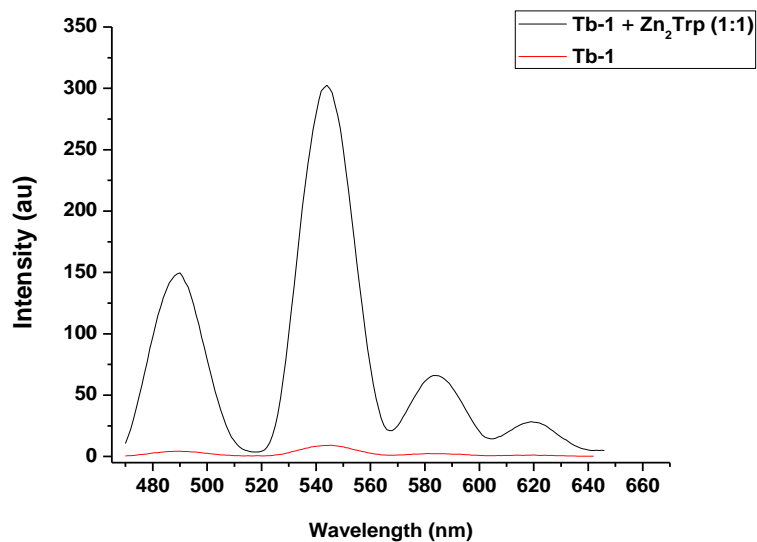


Figure S5: A comparison of **Tb-1** (2×10^{-5} M) intensity with and without **Zn₂Trp** in DSPC vesicles at 25 °C: [DSPC] = 1.6×10^{-4} M, [**Zn₂Trp**] = 2×10^{-5} M; λ_{ex} = 285 nm.

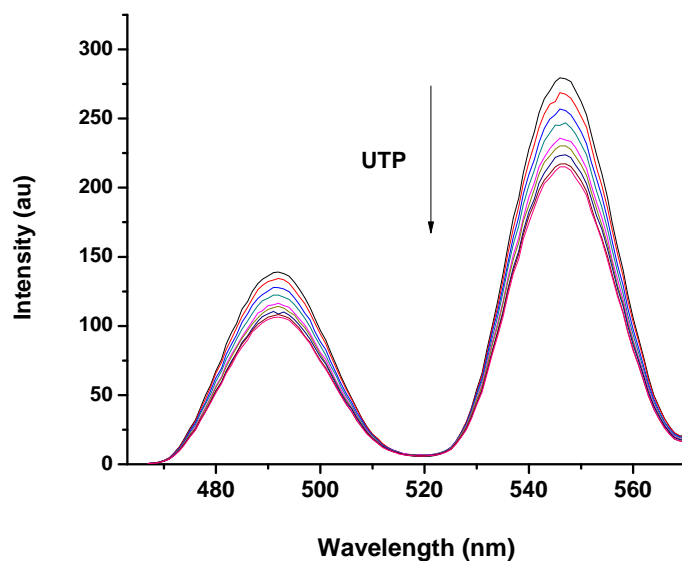


Figure S6. Emission titration (peaks at 490 nm and 544 nm are shown) of DPPC vesicles (1:2 ratio of embedded **Zn₂Trp** and **Tb-1**) vs UTP, ([DPPC] = 1.6×10^{-4} M), [**Zn₂Trp**] = 1.3×10^{-5} M, [**Tb-1**] = 2.6×10^{-5} M.

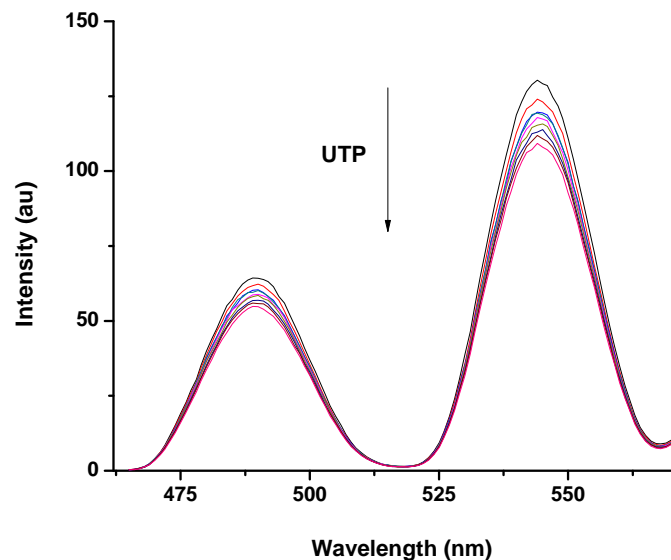


Figure S7. Emission titration (peaks at 490 nm and 544 nm are shown) of DPPC vesicles (2:1 ratio of embedded **Zn₂Trp** and **Tb-1**) vs UTP, ([DPPC] = 1.6×10^{-4} M), [**Zn₂Trp**] = 2.6×10^{-5} M, [**Tb-1**] = 1.3×10^{-5} M.

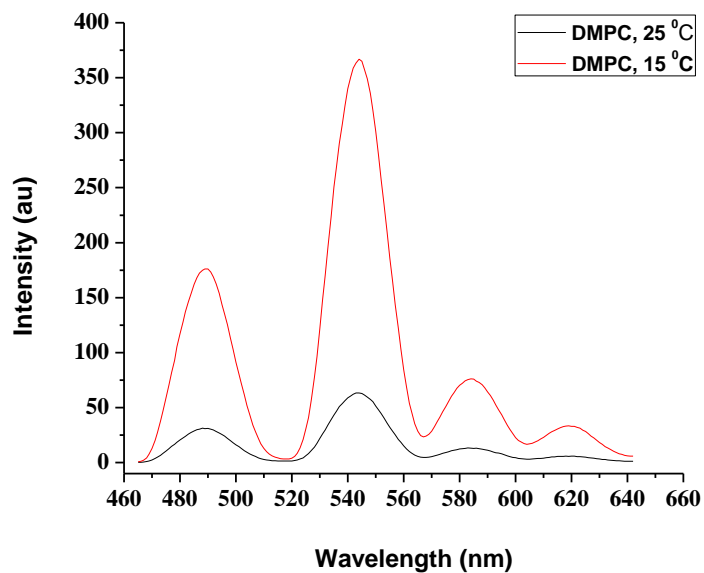


Figure S8. Emission intensity of **Tb-1** embedded in DMPC vesicles at different temperatures; vesicle composition: [DMPC] = 1.6×10^{-4} M, [**Zn₂Trp**] = [**Tb-1**] = 2×10^{-5} M, $\lambda_{\text{ex}} = 285$ nm.

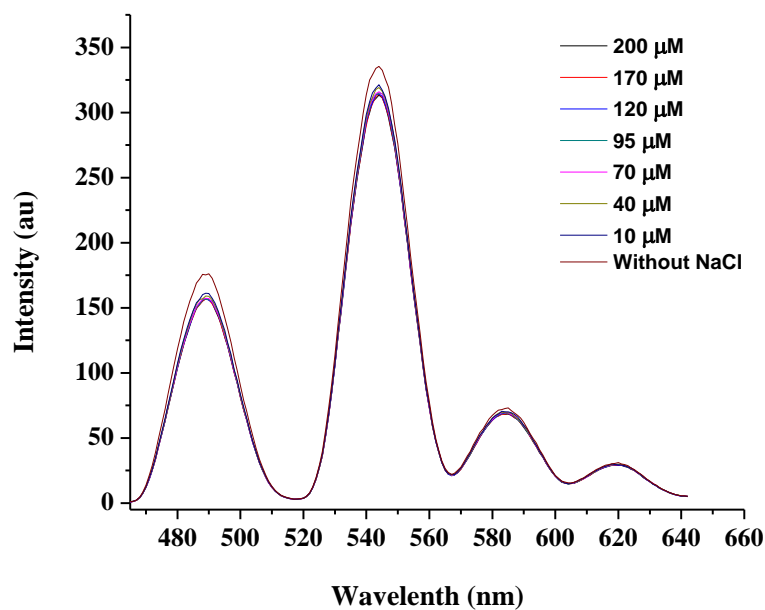


Figure S9. Emission change of DPPC vesicles upon NaCl addition at 25 °C: [DPPC] = 1.6×10^{-4} M, $[\text{Zn}_2\text{Trp}] = [\text{Tb-1}] = 2 \times 10^{-5}$ M; $\lambda_{\text{ex}} = 285$ nm.

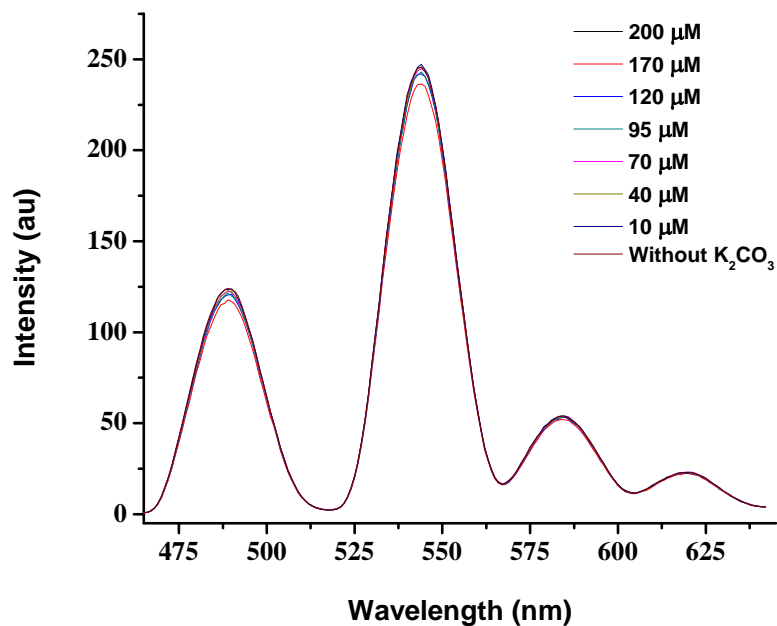


Figure S10. Emission change of DPPC vesicles upon addition of K_2CO_3 at 25 °C: [DPPC] = 1.6×10^{-4} M, $[\text{Zn}_2\text{Trp}] = [\text{Tb-1}] = 2 \times 10^{-5}$ M, $\lambda_{\text{ex}} = 285$ nm.

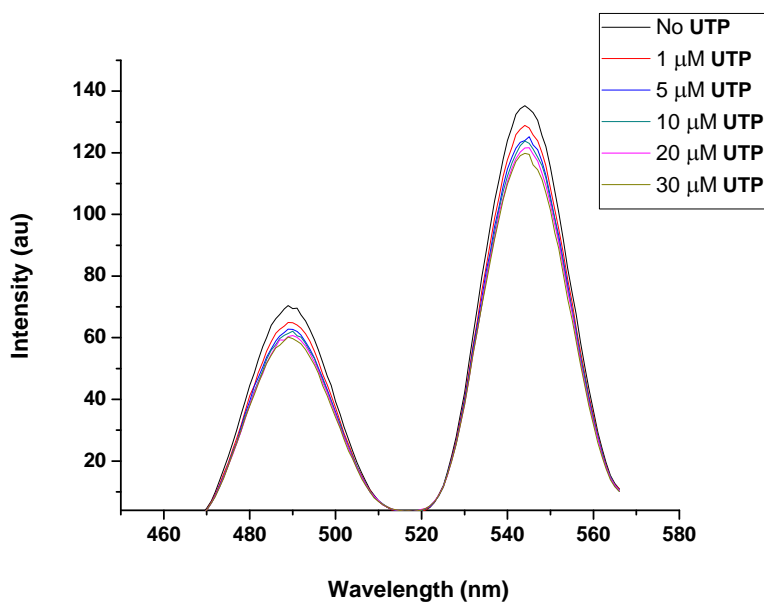


Figure S11. Change in emission intensity (peaks at 490 nm and 544 nm are shown) of **Tb-2** embedded DPPC vesicles (25 °C) upon addition of UTP: [DPPC] = 1.6×10^{-4} M, [Tb-2] = 2×10^{-5} M; λ_{ex} = 285 nm.

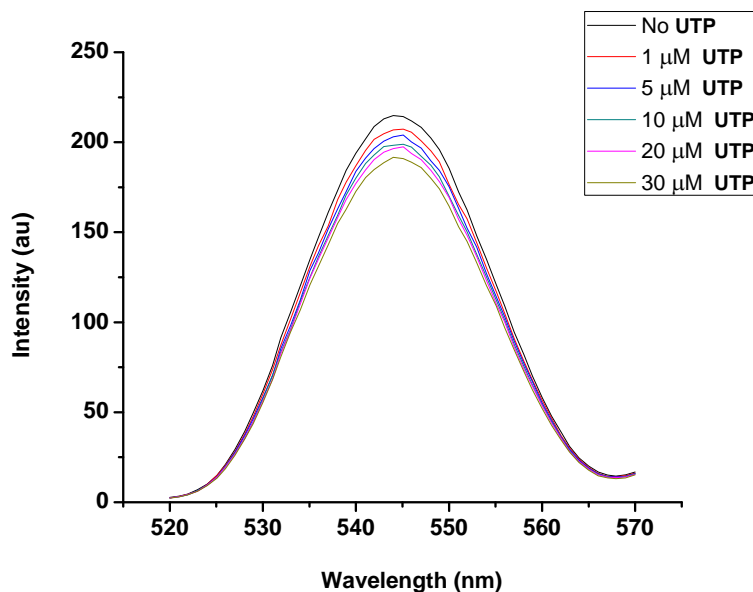


Figure S12. Change in emission intensity (peak at 544 nm is shown) of **Tb-2/Zn₂-C18** (1:1) co-embedded DPPC vesicles (25 °C) upon addition of UTP. [DPPC] = 1.6×10^{-4} M, [Tb-2] = [Zn₂-C18] = 2×10^{-5} M, λ_{ex} = 285 nm.

Excitation Spectra

The excitation spectra ($\lambda_{em} = 545$ nm) of vesicles embedded with **Tb-1** and **Zn₂Trp** resembled the absorption spectra of tryptophan chromophore suggesting the efficient sensitization Tb(III). After the addition of UTP or ATP, a decrease in the excitation bands was observed though the spectral pattern remained unchanged.

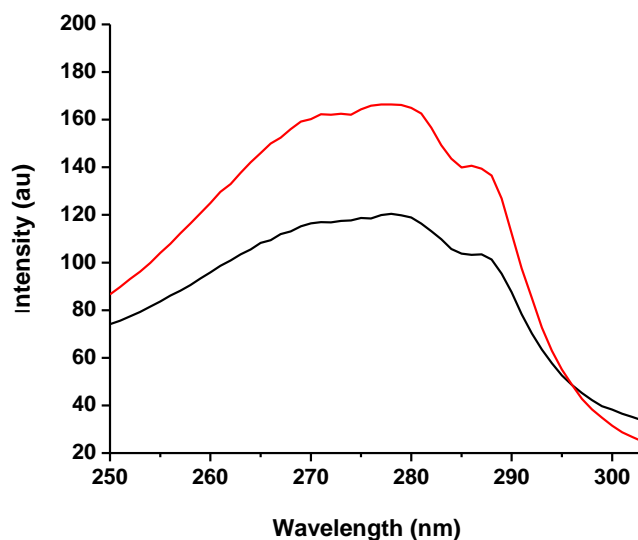


Figure S13. Excitation spectra ($\lambda_{em} = 545$ nm) of a DPPC vesicle co-embedded with **Tb-1/Zn₂Trp** (1:1) at 25 °C; before (red line) and after (black line) the addition of UTP (1.0 eqv). [DPPC] = 1.6×10^{-4} M, [Tb-1] = [Zn₂Trp] = 2×10^{-5} M.

Sensing of α -Casein

Proteins generally interact with vesicle surface through non-specific electrostatic interactions.⁷ To suppress these non-specific interactions and to gain selectivity for the phosphate anion zinc-cyclen receptor interaction, the vesicular surface was shielded by polyethylene glycol (PEG) residues. Therefore, vesicles were prepared from mixtures of DSPC and DSPE-PEG350 (1:1 mol ratio) having oligoethylene glycol residues attached to its polar head groups. These vesicles showed very negligible change upon addition of non-phosphorylated protein BSA, but showed a decrease in Tb(III) upon addition of α -Casein (though the response was poorer compared to the other phosphate anions).

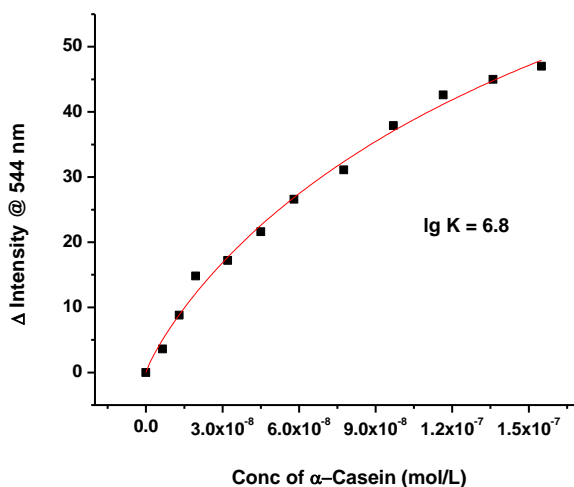


Figure S14. Binding curve of α -Casein against a DSPC/DSPE-PEG 350 (1:1) vesicle co-embedded with **Tb-1/Zn₂Trp** (1:1) at 25 °C; [lipid] = 1.6×10^{-4} M, [Tb-1] = [Zn₂Trp] = 2×10^{-5} M, λ_{ex} = 285 nm.

Size Exclusion Chromatography (SEC)

The bound analytes were removed from the vesicle solutions by size exclusion chromatography (SEC) small spin columns.⁸ For this Sephadex G-25 SEC medium was swollen in buffer solution for 3 hr prior to use. 3 mL bed volume per mL of vesicle suspension was transferred into a small plastic syringe with filter support (without a plunger) and the solvent removed by centrifugation (Eppendorf bench top centrifuge, 14 sec @ 4400 rpm). Vesicle solutions were subsequently added onto the column and filtered by centrifugation.

Hill Equation

$$\theta = [L]^n / (K_d + [L]^n)$$

where,

θ = the fraction of binding sites occupied

$[L]$ = the concentration of the free analyte

K_d = the dissociation constant

n = Hill coefficient

Non-linear fitting curves for different analytes (DPPC vesicles, 25°C)

Vesicle Composition: [DPPC] = 1.6×10^{-4} M, [Zn₂Trp] = 2×10^{-5} M, [Tb-1] = 2×10^{-5} M

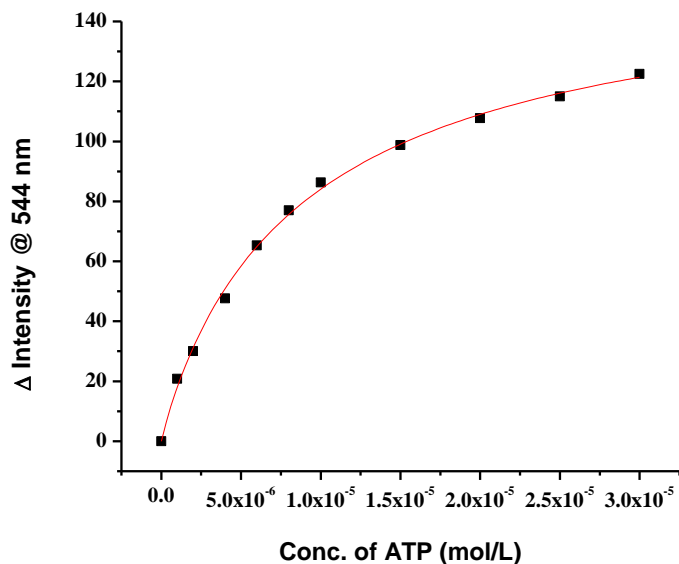


Figure S15. Binding curve for ATP

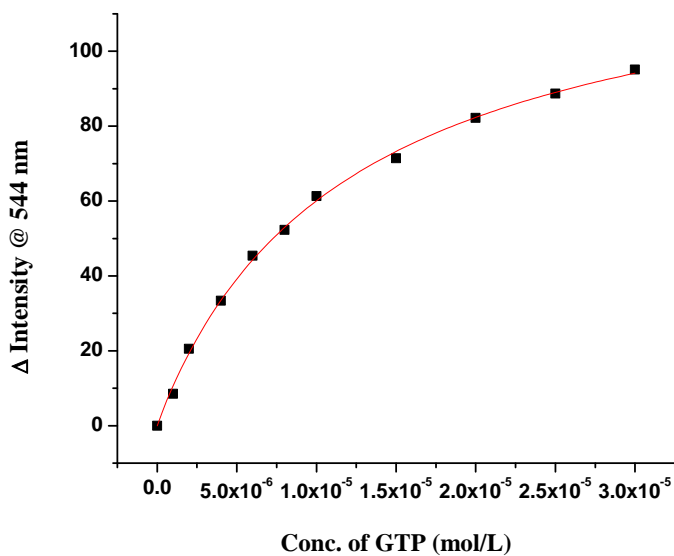


Figure S16. Binding curve for GTP

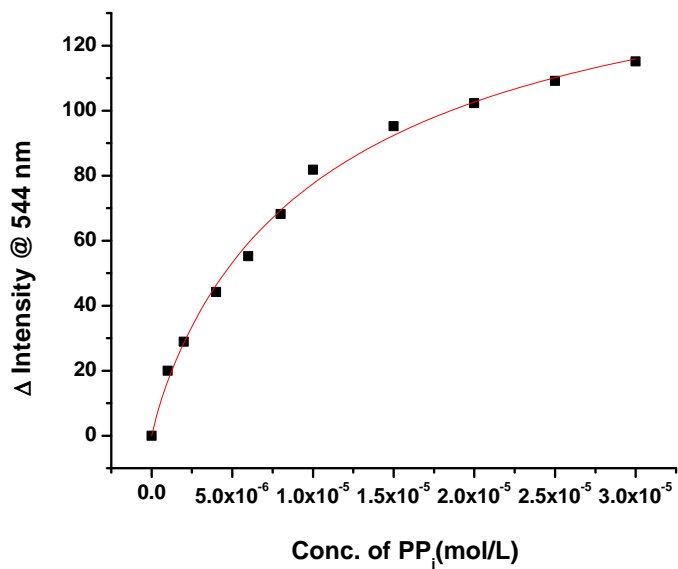


Figure S17. Binding curve for PP_i

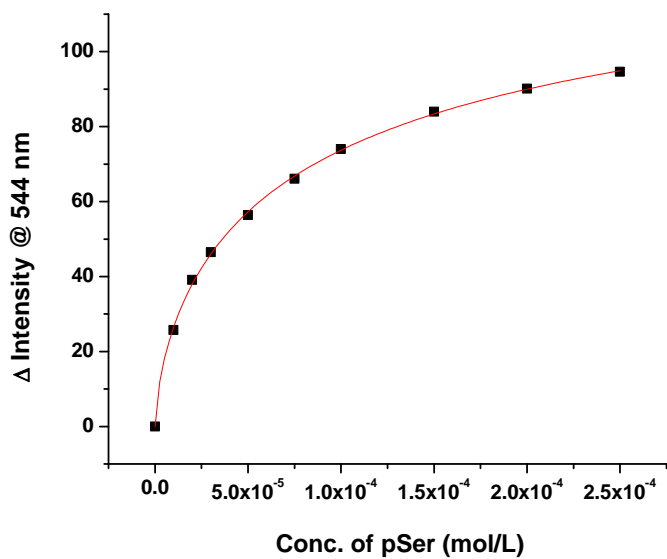


Figure S18. Binding curve for pSer

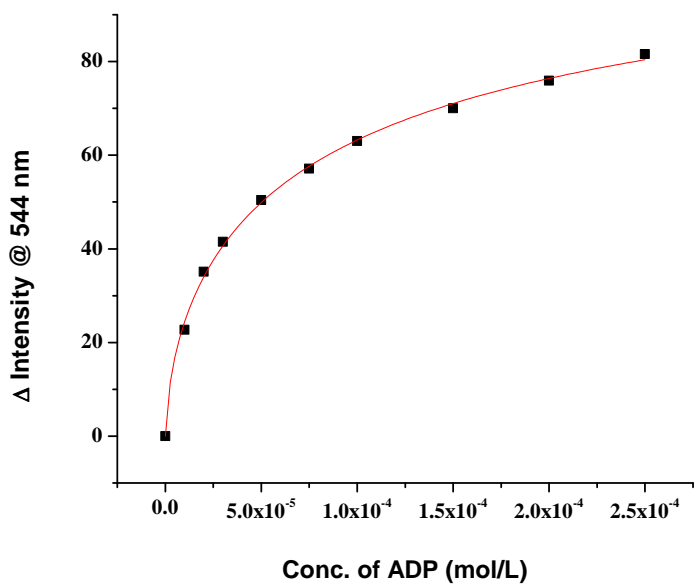


Figure S19. Binding curve for ADP

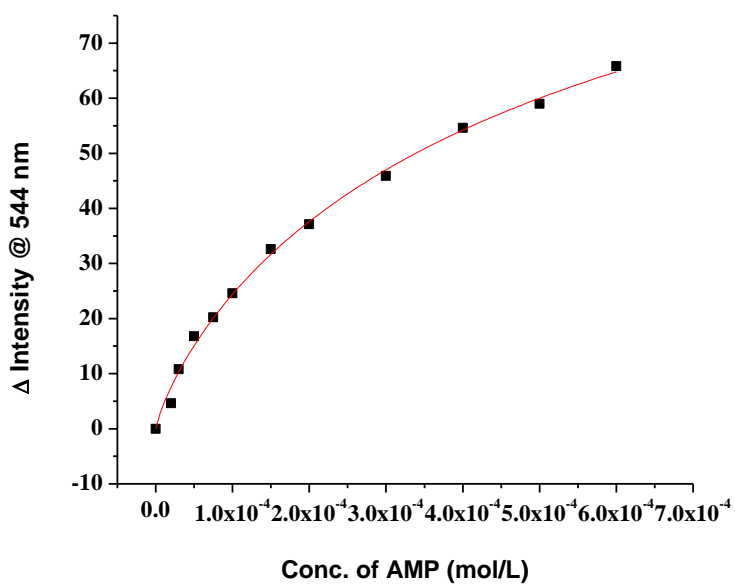


Figure S20. Binding curve for AMP

Comparison of binding constants of UTP and ATP between DSPC and DPPC vesicles at 25 °C

Table S2. Apparent binding constants of the **Zn₂Trp** receptor embedded in vesicles. ^aError in determining the binding constants values is ± 0.2 ; ^b These values are already listed in Table 1.

Lipid	Analyte	Binding Constant (lgK) ^a
1. DSPC	UTP	4.9
	ATP	4.8
2. DPPC	UTP	5.3 ^b
	ATP	5.2 ^b

Non-linear fitting curve for UTP against a DPPC vesicle (25 °C) after SEC

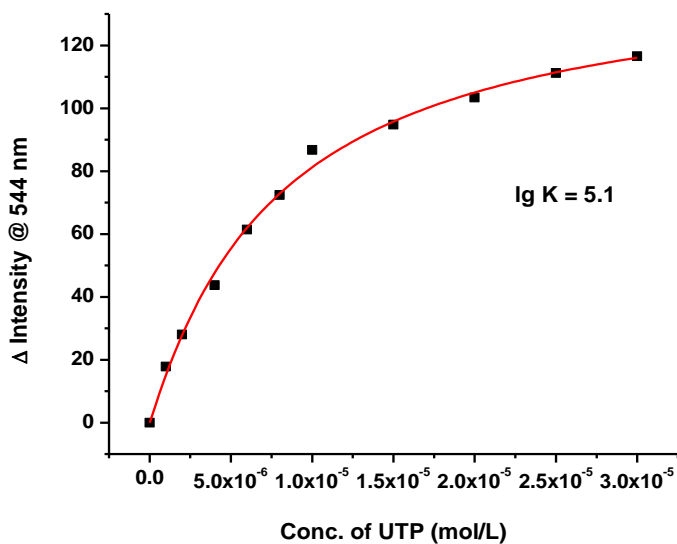


Figure S21. Binding curve for UTP

Non-linear fitting curves at other temperatures

Vesicle Composition: [lipid] = 1.6×10^{-4} M, [Zn₂Trp] = 2×10^{-5} M, [Tb-1] = 2×10^{-5} M

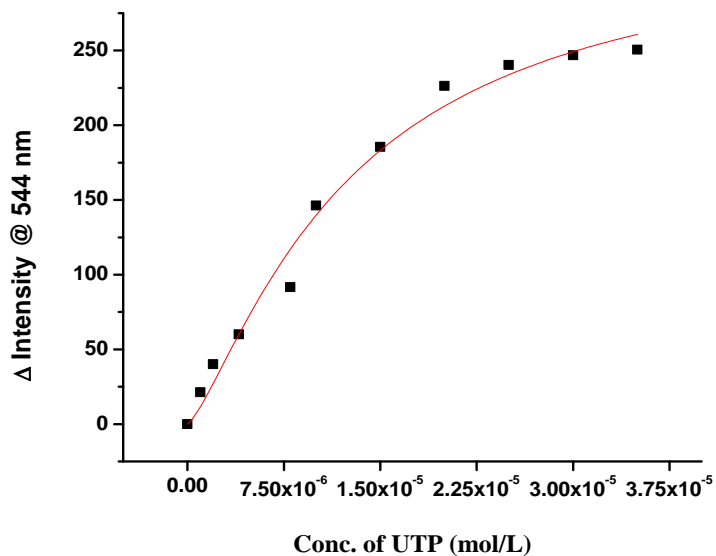


Figure S22. Binding curve for **UTP** at 15 °C against DMPC

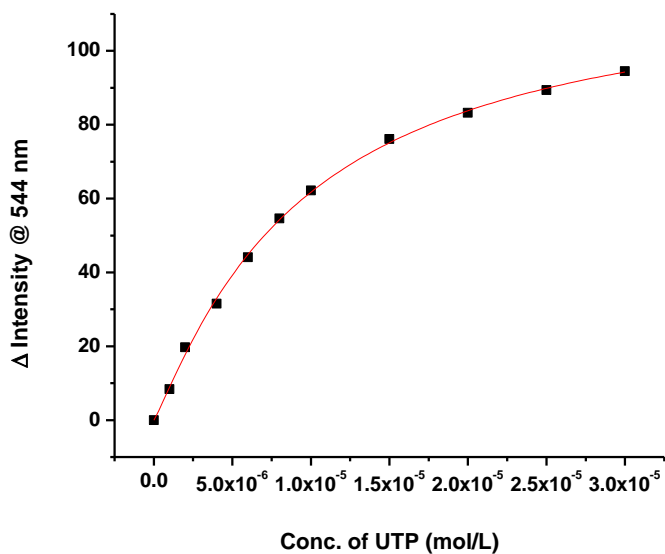


Figure S23. Binding curve for **UTP** at 37 °C against DSPC vesicles

References

1. D. S. Turygin, M. Subat, O. A. Raitman, V. V. Arslanov, B. König and M. A. Kalinina, *Angew. Chem., Int. Ed.*, 2006, **45**, 5340.
2. M. Bhuyan and B. König, *Chem. Commun.*, 2012, **48**, 7489.
3. C. L. Davies, N. G. Housden and A.-K. Duhme-Klair, *Angew. Chem., Int. Ed.*, 2008, **47**, 8856.
4. B. Gruber, S. Stadlbauer, A. Späth, S. Weiss, M. Kalinina and B. König, *Angew. Chem., Int. Ed.*, 2010, **49**, 7125.
5. A. I. Elegbede, M. K. Haldar, S. Manokaran, J. Kooren, B. C. Roy, S. Mallik and D. K. Srivastava, *Chem. Commun.* 2007, 3377.
6. (a) J. F. Nagle and S. Tristram-Nagle, *Biochim. Biophys. Acta*, 2000, **1469**, 159; b) P. Balgavy, M. Dubnickova, N. Kucerka, M. A. Kiselev, S. P. Yaradaikin and D. Uhrikova, *Biochim. Biophys. Acta*, 2001, **1512**, 40.
7. O. D. Velev, *Adv. Biophys.*, 1997, **34**, 139.
8. D. W. Fry, J. C. White and I. D. Goldman, *Anal. Biochem.*, 1978, **90**, 809.